

Review

Inputs of Numerical Simulation into the Development of Shock Adhesion Tests on Advanced Materials

Michel Arrigoni

IRDL UMR CNRS 6027, ENSTA BRETAGNE, Brest, France

Article history

Received: 27-11-2019

Revised: 21-12-2019

Accepted: 09-01-2020

E-mail: Michel.arrigoni@ensta-bretagne.fr

Abstract: Advanced materials- such as assemblies, composites and materials obtained by additive methods - have met a great success in the industry of advanced technologies. They allow combining a variety of different materials and following sophisticated geometries. However, their mechanical behavior, bulk as well as in assembly, remains to be better understood to assess their reliability. For this reason, laser induced shock tests have encountered an increasing interest for this last decade. They started with the determination of the spallation damage threshold and have been extended to the bond strength evaluation of adhesively bonded assembly, thick coatings and many configurations for a variety of applications. By the use of this laser induced shock wave process, experiments were carried out and results were explained by analytical studies and 1D hydrodynamic simulation first. But rapidly, 2D and 3D simulations were necessary to explain phenomenon occurring during wave propagation in complex situations, like fracture, attenuation. This work shows some examples treated during the development of the LASer Adhesion Test (LASAT) that relies on laser induced shock wave propagation. During these developments, inverse approach by finite element analysis with explicit method allows understanding the recorded experimental signals showing fracture and adhesion evaluation in tested sample. The numerical code RADIOSS® is used to evaluate stresses and energy dissipation at the interface, as well as for understanding edge effects and attenuation. This article proposes an overview of the work performed with finite element methods in explicit scheme correlated to laser induced shock wave experiments.

Keywords: Additive Methods, Coating, Adhesion, LASAT, FEM

Introduction

During the last fifteen years, additive methods have met a great step towards the industry of advanced technologies that promises to be fruitful. In addition to manufacture complex geometries, Jeandin *et al.* (2010) showed that additive methods such as plasma spraying technique also allow the association of different materials having complementary properties. Barbezat (2001), Guipont *et al.* (2010) gave significant illustrative examples, not only in the frame of automotive industry but also for medical applications like hip prosthesis. Nowadays, additive manufacturing methods even start to be accessible to citizens. However, materials obtained by 3D manufacturing and additive methods are not mechanically equivalent to the same monolithic material. In order to assess their reliability and also to estimate their adhesion on substrate, the Laser Shock Adhesion Test has been experienced by Barradas *et al.* (2004) and detailed

by Bolis *et al.* (2007) on the basis of the laser induced shock wave. This process consists in controlling and evaluating the adhesion of a coating on its substrate Fig. 1.

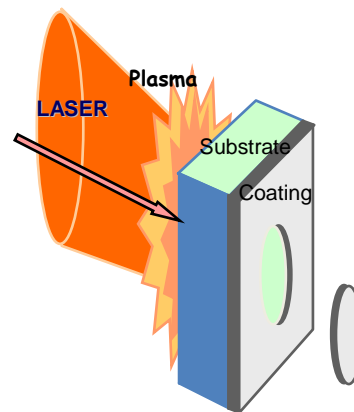


Fig. 1: Principle of the LASAT test.

The LASAT Process

A good adhesion of the coating is crucial for insuring a safe use in service of 3D printed devices. A first review of the LASAT process was previously proposed by Berthe *et al.* (2011).

Thus, in order to check the adhesion of a printed material on its substrate, adhesion tests were developed. However, solicitations involved in the diversity of existing tests might differ from one test to another; they can be under unimodal or mixed mode, dynamic or quasi-static, making difficult comparisons and interpretations of results. Besides, some tests consider the mounting of the tested sample in a frame or clamping system, like the bond pull test, that is not convenient for high pace testing. The LASAT process brings a suitable alternative. Indeed, it is a contactless technique based on laser use for generating the stress, as well as for measuring the shock effects and thus, it is automatable. Barradas *et al.* (2004) proposed a concept based on spallation phenomena under dynamic solicitation applied at the additive material coating-substrate interface. Spallation is a crack occurring inside the material, depending on the wave propagation and resulting from dynamic tensile stress. It is explained by the coincidence of two release waves during waves propagation: A shock wave followed by a release wave propagate both towards the coating free surface. When the shock wave reaches the coating free surface, it is reflected as a release wave towards the loaded surface and thus, crosses the incident release wave. This situation gives birth to a uni-axial traction state noted $n^{\circ}4$ on Fig. 2. This traction state propagates within the sample and reaches the coating-substrate interface and, according to its intensity, may lead to an interfacial crack Fig. 3, resulting from spallation.

The tensile stress available at the coating - substrate interface depends on the shock loading. A power pulsed laser brings into play the incident energy for creating a shock. Indeed, the focused laser beam sublimates a thin part of the substrate, engendering the expansion of plasma. According to action-reaction principle, this plasma pushes in the direction of the target, resulting in shock wave propagation through the sample thickness. The shock propagation can be monitored from the free surface by the use of another laser, a continuous one, focused on the coating free surface as a Doppler interferometer probe, named Velocity Interferometer System for Any Reflectors (VISAR) detailed by Barker *et al.* (1972). This device allows recording the coating free surface velocity during the experiment, Fig. 4. These records give information not only about the shock intensity but also about the interface integrity as an ultra-fast diagnostic tool, as described by Bolis *et al.* (2007). A good agreement of this recorded signal with numerical simulation allows obtaining the stress history at the coating substrate interface by inverse approach. This inverse approach is based on minimizing the simulated free surface velocity relative to the experimental signal by the method of least squares. The modified input data is the maximum pressure that remains in the uncertainty range. Pressure is deduced by the measurement of the laser energy and the irradiated surface according to Berthe *et al.* (1997). Then, a practical adhesion work is deduced. Arrigoni *et al.* (2006) proposed a comparative study that evaluates the relevance of the LASAT test compared to bulge-and-blister test and bond pull test and that resulted in the same discrimination of various adhesion qualities of plasma sprayed copper on aluminium substrate.

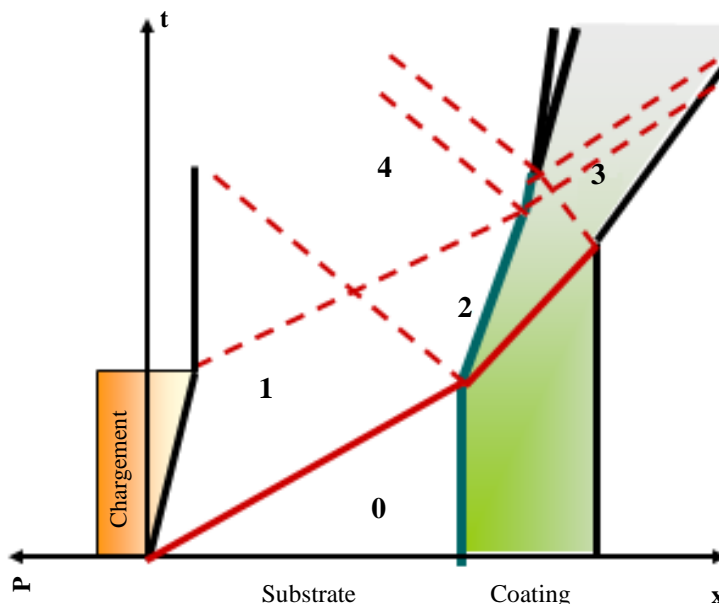


Fig. 2: Space-time diagram of a shock propagation in a biomaterial target



Fig. 3: Cross section analysis of a Cr 110 μm-Cu 90 μm sample after LASAT test

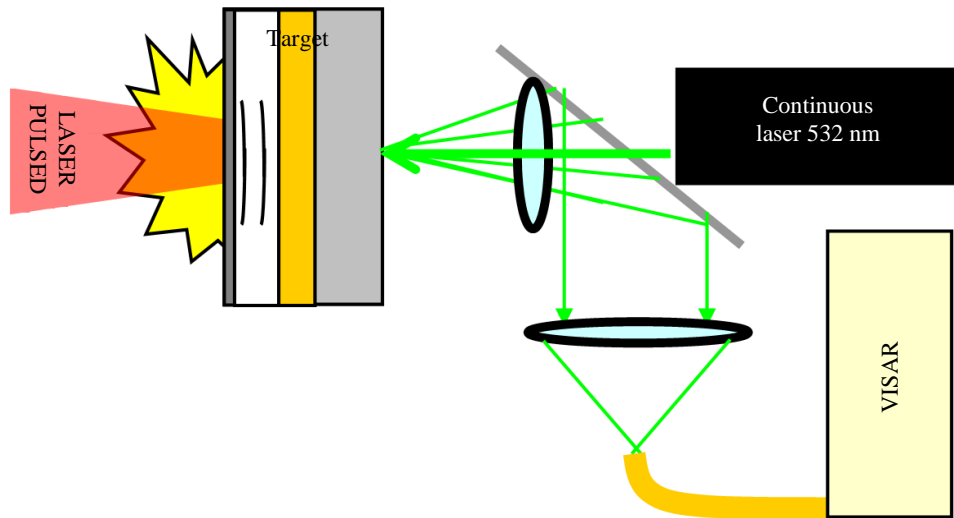


Fig. 4: Scheme of the LASAT process

LASAT Transposition in Industry

Barradas *et al.* (2005) showed that despite of its efficiency in some coating/substrate samples, laser adhesion tests meet some limitations for their implementation in industry, which can be, for example, the high cost of laser sources able to test thick samples, the sensitivity of the shock wave to its propagation medium including porosity and roughness at the coating/substrate interface for instance. Research works focused then on three topics: the influence of the coating/substrate roughness, of the porosity and alternative solutions for thicker or multi-layered samples.

Modelling of Porous Materials Under Dynamic Loading

The mechanical behavior of materials obtained by additive manufacturing processes, like thermal spraying, is dependent of porosity, inherent to the manufacturing process. It is then necessary to characterize the material behavior in order to extend LASAT from a simple quality test to a quantitative measurement of the traction at the origin of the disassembling. Arrigoni *et al.* (2007) performed compaction modelling on sintered steel Distaloy AE and thermal sprayed copper (Arrigoni *et al.* (2008a). This has led to an analytical and macroscopic $P(\alpha)$ -like model, named toboggan, describing the residual compaction during the shock compression. This model

implemented as a Fortran subroutine in the hydrodynamic code RADIOSS®. This software provided in the Altair Hyperworks software suite is a finite element code including an explicit solver. It is able to give a good agreement with experimental signal obtained on laser induced shock experiments, with a VISAR, on 14% porous plasma sprayed copper, Fig. 5. During shock propagation, compression obeys to the shock equation of state Equation 1 and in release phase to the Mie-Grüneisen equation of state Equation 2. The assumption of invariance of the ratio of the Grüneisen coefficient over the specific volume is done Equation 3:

$$D = c_0 + s.(u - u_0) \quad (1)$$

$$P(E, v) - P_{ref}(E, v) = (\Gamma / v)(E - E_{ref}) \quad (2)$$

$$\frac{\Gamma}{v} = \frac{\Gamma_0}{v_0} = Cte \quad (3)$$

Where:

- D = The shock velocity, u refers to the material velocity, C_0 is the bulk sound velocity and s is the Hugoniot parameter
- P = The hydrodynamic pressure and P_{ref} is a state of reference that can be either the Hugoniot plateau or the cold state at 0°K

$v = 1/\rho =$ Specific volume that is the inverse of density. Subscript $_0$ refers to initial density. E stands for internal energy and Γ is the Grüneisen coefficient

It is a classical approach in shock physics. The reader who wants to extend his knowledge about shock physics can refer to Meyers (1994). The mechanical loading resulting from the laser-matter interaction has been deduced by the use of ESTHER code described by Bardy *et al.* (2016) and is illustrated in Fig. 6.

The target is considered free (no boundary condition) during the calculation. Even though it was set on a washer during experiments, the observation time is too short for perceiving the effects of the waves coming back from the edge of the target. Material parameters are given in Table 1.

Influence of the Interfacial Roughness

Arrigoni *et al.* (2006) applied the LASAT process to plasma sprayed copper coatings on aluminium substrate allowed to discriminate adhesion level due to sample preparation. Interfacial roughness, cleanness and temperature are key parameters on the adhesion obtained after spraying. In order to take into account the effects of the interfacial roughness on the tensile stress during the wave propagation, a regular interface roughness in “saw teeth” was prepared by milling. Observations of cross section of polished recovered samples after laser induced shock experiments, by the use of optical microscopy, shows that the crack is located near the head of the

roughness on the longer side Fig. 6a. Nondestructive ultrasonics or xray tomography would have been a better alternative but not available at the time of this study. However, the LASAT technique was successfully utilized for the interface debonding of adhesively bonded aluminium plates when the laser was operated in ablative regime. At much lower laser intensity, the laser can be utilized as an ultrasonic source. This technique was indeed used by Arrigoni *et al.* (2008b) as a nondestructive technique for Bond inspection by Bscan.

A 2D numerical approach performed with the code RADIOSS®, revealed that computed tensile stresses along the roughness are composed of shear stress σ_t (mode II) and normal stress σ_n (mode I). The location of maximal stresses at the interface Fig. 6b, c corresponds to the location of the crack observed on the cross section of the recovered sample after shock. A red horizontal line marks the cutoff limit that permits to reproduce the interfacial fracture on trials. The constitutive law adopted for the Al 2017 substrate is a “perfect elastoplastic” model without considering viscous effects as a first approach. Material parameters are given in Table 1.

Table 1: Material properties

Material	C_0 m/s	ρ_0 kg/m ³	Γ	s	Y_0 MPa
Plasma sprayed copper (Arrigoni <i>et al.</i> , 2007)	3490	7680	2	1.49	90
Al 2024 substrate (Meyers, 1994)	5350	2700	2	1.339	120

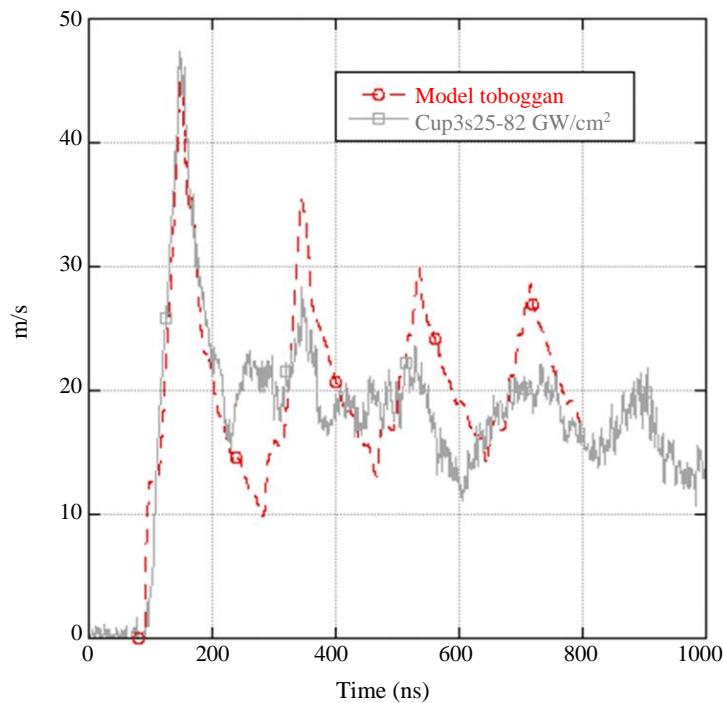


Fig. 5: Comparison between experiment and numerical simulation of the record of the free surface velocity after impact at 82 GW/cm² on plasma sprayed copper, 14% porous

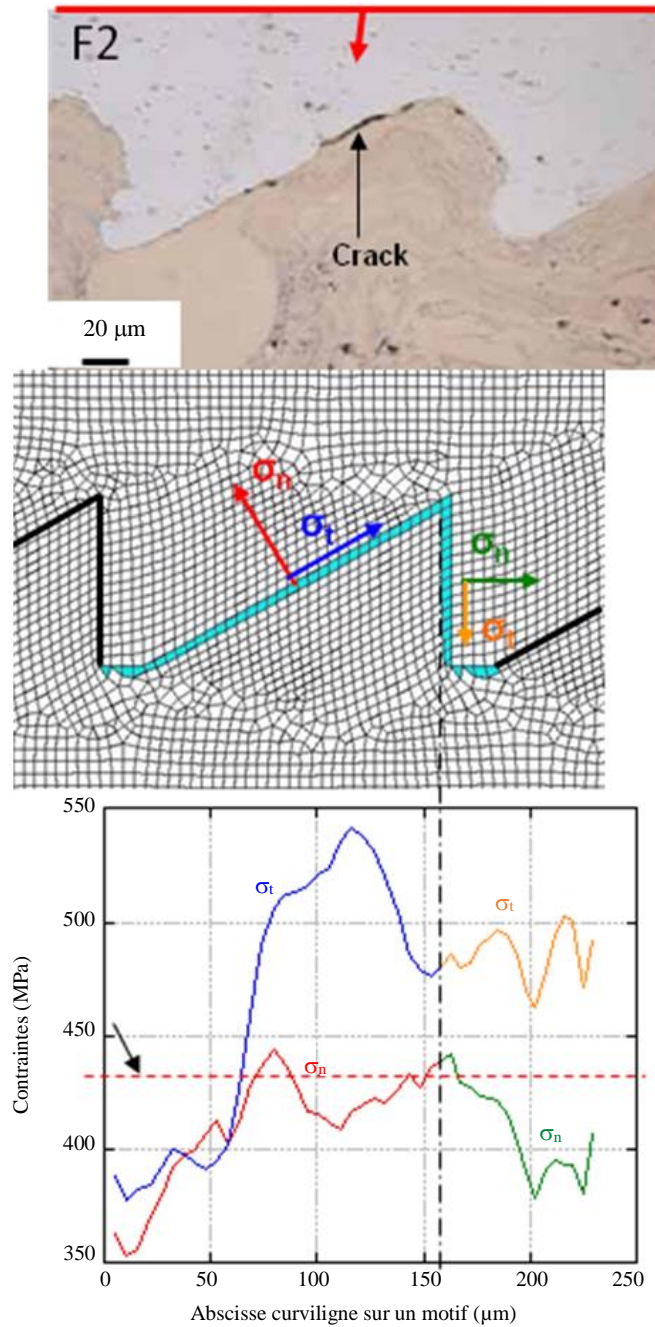


Fig. 6: (a) Post-mortem analysis; (b) Mesh and geometry; (c) Computed stresses

Edge Effects

Spallation of materials induced by laser driven shock waves is generally produced under uniaxial (one-Dimensional (1D)) deformation by irradiating a spot of diameter much greater than the sample thickness. Here, edge effects are occurring in shock wave propagation by drastically reducing the loaded spot. Experiments performed on aluminium samples detect the effect of

lateral wave propagation, both on recovered samples and on time-resolved VISAR measurements. Damage zones are localized completely differently from that under uniaxial condition, according to the presence of edge effects and the signature of these edge effects can be read on VISAR signals. Numerical simulations with RADIOSS® provide a full understanding of wave propagation and resulting damage in 1D or 2D-axisymmetric configuration (Boustie *et al.* 2007).

Comparisons with experimental VISAR signals show the possibility of validating more accurately the dynamic damage criteria, including the edge effects Fig. 7.

LASAT for Composite Materials

The LASer Adhesion Test (LASAT) technique originally developed for testing the adhesion of coatings on various substrates has been applied to laminated long carbon fiber reinforced epoxy unidirectional laminates stacked in 1, 4 or 8 oriented plies of G40-800 carbon fibers with Cytec 5276-1 epoxy resin, ranging from 125 μm to 1500 μm in total thickness.

High power laser irradiation with different intensities below 1500 GW/cm^2 has been applied to these different laminates. The propagation of shock waves into these targets results in the generation of tensile stress, resulting in cracks within the plies (intra-laminar delamination) or full delamination at their interface in the interply layer

(inter laminar delamination). At high intensity, fractures are localized both near the loading zone and near the opposite face. In order to interpret and understand these experimental observations, a numerical study with the code RADIOSS® was carried out by Boustie *et al.* (2010). It consists of a simplified composite target model in which four isotropic plies are represented by a layered sandwich material with alternating layers of epoxy interply and carbon fiber. The dynamic behaviour of each layer is described by a hydrodynamic elasto-plastic model where the hydrodynamic component of the stress tensor is calculated through the relationship:

$$P = C_0 + C_{1\mu} + C_{2\mu^2} + C_{3\mu^3} + (C_4 + C_{5\mu})(E - E_0) \quad (4)$$

where, $\mu = 1 - \rho/\rho_0$ and E is the internal energy, using the data of Table 2.

Table 2: Composite material properties

	Epoxy resin	Carbon
Density ρ_0 (g/cm^3)	1.2000	1.7900
Young modulus (Mbar)	0.5200	1.6260
Poisson ratio	0.3800	0.3000
Sound speed c_0 ($\text{cm}/\mu\text{s}$)	0.2788	0.4197
S (in $D = c_0 + s.u$, D: Shock speed, u material velocity)	1.3921	1.6677
Γ , Mie Grüneisen coefficient	1.0000	2.0000
$C_1 = \rho_0.c_0^2$	0.0930	0.3990
$C_2 = \rho_0.c_0^2(2s-1-\Gamma/2)$	0.1190	0.5330
$C_3 = \rho_0.c_0^2((s-1)(3s-1)-\Gamma/2(2s-1))$	0.0330	0.1350
$C_4 = C_5 = \Gamma \cdot \rho_0$	1.2000	4.5300

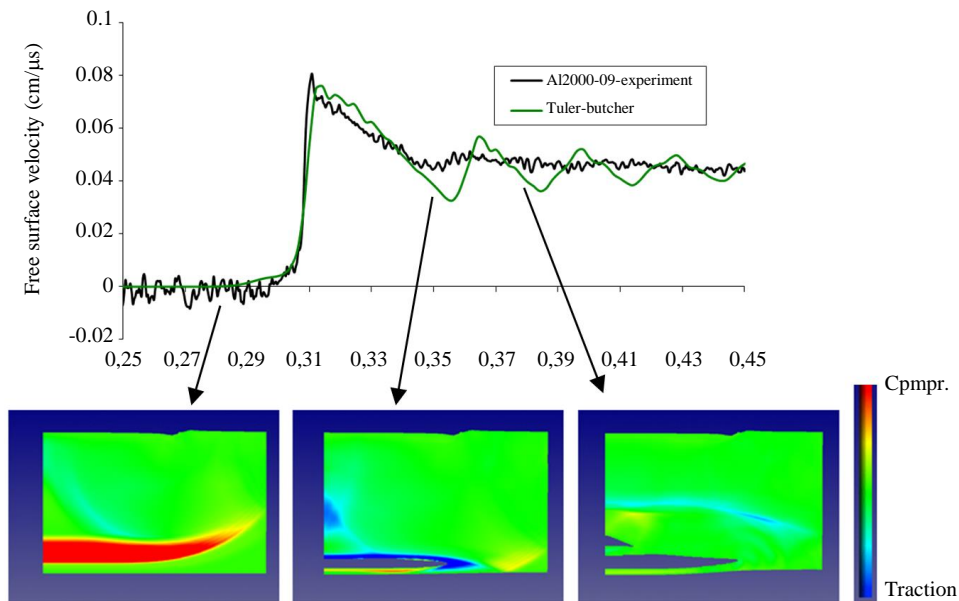


Fig. 7: Comparison of experimental velocity signals and corresponding numerical simulation with Tuler-Butcher damage criterion for (a) Al 2 mm thick, spot diameter: 4 mm, $\tau = 5 \text{ ns}$, $I = 2.08 \text{ TW}/\text{cm}^2$ -pictures of pressure and damage repartition calculated by RADIOSS® (Boustie *et al.*, 2007)

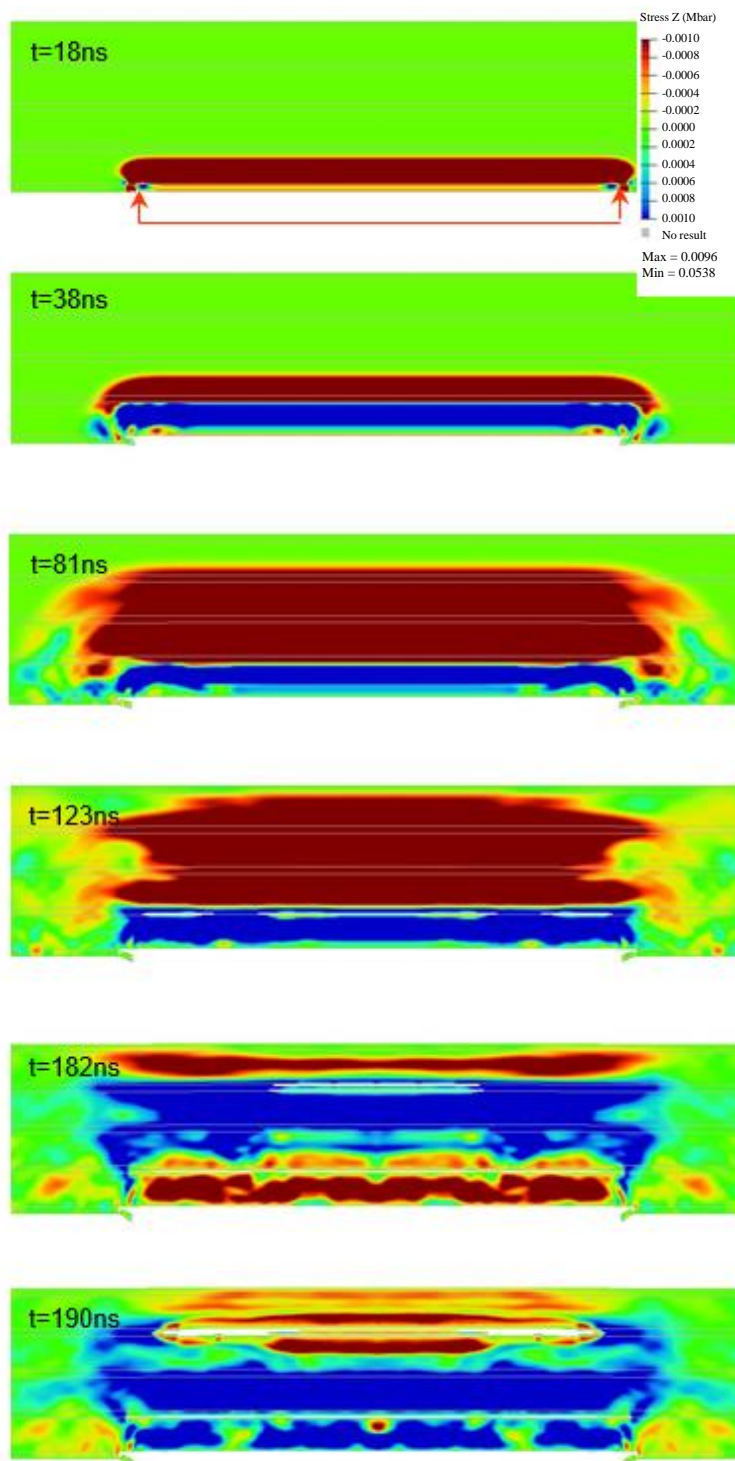


Fig. 8: RADIOSS® numerical simulation of laser shock propagation (axial stress, compression in red, tension in blue) in a 4 ply laminates according to data of Table 1 with a peak pressure of 5 GPa and resulting in damage in the composite

This model allows understanding of the origin and location of stresses produced in the material and the resulting observed fractures Fig. 8. The loading is applied

on a 2 mm diameter and the amplitude of the loading is dependent on the laser intensity and estimated through the Grün law (Grün *et al.*, 1981) as a first approximation.

In order to predict damage location, a “cut-off” fracture model was used; giving an arbitrary value to the strength of each material equals to double its elastic limit. For a peak pressure loading of 5 GPa, the shock wave propagation results in tensile load near the loaded zone before the shock has reached the back surface.

The direction of the cracks produced is mainly parallel to the layers interfaces in fine. This shows that the tensile stress is also due to the transmission/reflection of shock waves at the interface between each material. Due to the impedance mismatch between epoxy and carbon, shock waves can be reflected as release waves whose crossing can result in fracture enhanced by an arbitrary choice of a low value for the rupture threshold.

This could explain the presence of fractures near the loading zone. Later, the main shock wave reverberates at the free surface and produces tensile loads sufficient to produce delamination Fig. 8c, with the final result being a sample fractured both near the front and the back surfaces as observed experimentally.

With these very simplified assumptions, we can only give qualitative indications of what happens inside the target, not at all quantitative ones. In addition to post mortem observation, time-resolved data as back free-surface velocity time history should be gathered with different levels of shocks in order to predict the complex damage modelling of this material. Indeed, anisotropy of the material has been accounted for in shock wave propagation by Ehrhart *et al.* (2014).

Conclusion

Progresses have been done in the modelling of the behavior of porous materials under shock, in the shock response of a rough interface, in the edge effects associated to the shock propagation. These results allow understanding experimental results that can be correlated to numerical simulation. The inverse approach using the RADIOSS® code gave some quantitative results. These improvements allow extending the LASAT process to a larger range of industrial samples for a qualitative study as well as for a quantitative stress measurement. It has notably been extended to composites and adhesively bonded materials. The LASAT process is also able to test thick samples as well as thin film.

Acknowledgement

Authors would like to thank the PPRIME, PIMM and C2P technical and administrative staff for their helpful participation and industrial partners: APS Pletech (Marne La Vallée, France), KME Tréfilimétaux (Sérifontaine, France), Sulzer Metco (Wohlen, Switzerland), GIE REGIENOV (Guyancourt, France), CEA and ALTAIR-group for their kind support on RADIOSS® code. Authors would also like to thank

the Institute of Aerospace Research of the National Research Council of Canada for having provided composite samples.

Funding Information

This study has been started through the LASAT project supported by the French Ministry of Scientific Research and Education through the “Materials and Processes Network” and then continued within a Franco-Canadian project named SATAC.

Ethics

Author has no ethical issues that may arise after the publication of this manuscript.

References

- Arrigoni, M., S. Barradas, M. Braccini, M. Dupeux and M. Jeandin *et al.*, 2006. A comparative study of three adhesion tests (EN 582, similar to ASTM C633, LASAT (LASer Adhesion Test) and bulge and blister test) performed on plasma sprayed copper deposited on aluminium 2017 substrates. *J. Adhesion Sci. Technol.*, 20: 471-487. DOI: 10.1163/156856106777144336
- Arrigoni, M., M. Boustie, T. De Resseguier, F. Pons and H.L. He *et al.*, 2007. Use of a macroscopic model for describing the effects of porosity on shock wave propagation. *J. Applied Phys.*, 101: 083514-083514. DOI: 10.1063/1.2718868
- Arrigoni, M., M. Boustie, C. Bolis, L. Berthe and S. Barradas *et al.*, 2008a. The use of a macroscopic formulation describing the effects of dynamic compaction and porosity on plasma sprayed copper. *J. Applied Phys.*, 103: 083509-083509. DOI: 10.1063/1.2906186
- Arrigoni, M., Q. Hu, M. Boustie, L. Berthe and J.P. Monchalin, 2008b. B-scan simulations with abaqus for laser ultrasonic inspection of structures. *Proceedings of the 1st International Symposium on Laser Ultrasonics: Science, Technology and Applications, Montreal, (TAM' 08)*, pp: 1-6.
- Barbezat, G., 2001. The state of the art of the internal plasma spraying on cylinder bore in AlSi cast alloys. *Int. J. Automotive Technol.*, 2: 47-52.
- Bardy, S., B. Aubert, L. Berthe, P. Combis and D. Hébert *et al.*, 2016. Numerical study of laser ablation on aluminum for shock-wave applications: development of a suitable model by comparison with recent experiments. *Opt. Eng.*, 56: 011014-011014. DOI: 10.1117/1.OE.56.1.011014
- Barker, L.M. and R.E. Hollenbach, 1972. Laser interferometer for measuring high velocities of any reflecting surface. *J. Applied Phys.*, 43: 4669-4675. DOI: 10.1063/1.1660986

- Barradas, S., M. Jeandin, C. Bolis, L. Berthe and M. Arrigoni *et al.*, 2004. Study of adhesion of PROTAL® copper coating of Al 2017 using the Laser Shock Adhesion Test (LASAT). *J. Mater. Sci.*, 39: 2707-2716.
DOI: 10.1023/B:JMSE.0000021445.74736.b3
- Barradas, S., R. Molins, M. Jeandin, M. Arrigoni and M. Boustie *et al.*, 2005. Application of laser shock adhesion testing to the study of the interlamellar strength and coating-substrate adhesion in cold-sprayed copper coating of aluminum. *Surface Coatings Technol.*, 197: 18-27.
DOI: 10.1016/j.surfcoat.2004.08.222
- Berthe, L., M. Arrigoni, M. Boustie, J.P. Cuq-Lelandais and C. Broussillou *et al.*, 2011. State-of-the-art Laser Adhesion Test (LASAT). *Nondestructive Test. Evaluat.*, 26: 303-317.
DOI: 10.1080/10589759.2011.573550
- Berthe, L., R. Fabbro, P. Peyre, L. Tollier and E. Bartnicki, 1997. Shock waves from a water-confined laser-generated plasma. *J. Applied Phys.*, 82: 2826-2832. DOI: 10.1063/1.366113
- Bolis, C., L. Berthe, M. Boustie, M. Arrigoni and S. Barradas *et al.*, 2007. Physical approach to adhesion testing using laser-driven shock waves. *J. Phys. D: Applied Phys.*, 40: 3155-3155.
DOI: 10.1080/10589759.2011.573550
- Boustie, M., E. Gay, L. Berthe, M. Arrigoni and J. Radhakrishnan *et al.*, 2010. LASER Shock Adhesion Test (LASAT) of composite materials for aerospace industry. *Proceedings of the 23rd International in Conference on Surface Modification Technologies, (SMT' 10)*, pp: 2-5.
- Boustie, M., J.P. Cuq-Lelandais, C. Bolis, L. Berthe and S. Barradas *et al.*, 2007. Study of damage phenomena induced by edge effects into materials under laser driven shocks. *J. Phys. D: Applied Phys.*, 40: 7103-7103.
DOI: 10.1088/0022-3727/40/10/019
- Ehrhart, B., R. Ecault, F. Touchard, M. Boustie and L. Berthe *et al.*, 2014. Development of a laser shock adhesion test for the assessment of weak adhesive bonded CFRP structures. *Int. J. Adhesion Adhesives*, 52: 57-65.
DOI: 10.1016/j.ijadhadh.2014.04.002
- Grun, J., R. Decoste, B.H. Ripin and J. Gardner, 1981. Characteristics of ablation plasma from planar, laser-driven targets. *Applied Phys. Lett.*, 39: 545-545. DOI: 10.1063/1.92788
- Guipont, V., M. Jeandin, S. Bansard, K.A. Khor and M. Nivard *et al.*, 2010. Bond strength determination of hydroxyapatite coatings on Ti-6Al-4V substrates using the LASER Shock Adhesion Test (LASAT). *J. Biomed. Mater. Res. Part A*, 95: 1096-1104.
DOI: 10.1002/jbm.a.32907
- Jeandin, M., D. Christoulis, F. Borit, M.H. Berger and S. Guetta *et al.*, 2010. Lasers and thermal spray. *Mater. Sci. Forum*, 638: 174-181.
DOI: 10.4028/www.scientific.net/MSF.638-642.174
- Meyers, M.A., 1994. *Dynamic Behavior of Materials*. 1st Edn., John Wiley and Sons, ISBN-13: 9780471582625.